Nucleic Acids Research, 2005, Vol. 33, No. 19 ***e170***
doi:10.1093/nar/gni171

In vitro non-viral gene delivery with nanofibrous scaffolds

Dehai Liang[1], Yen K. Luu[2], Kwangsok Kim[1], Benjamin S. Hsiao[1,2], Michael Hadjiargyrou[2] and Benjamin Chu[1,2,3,*]

[1]Department of Chemistry, Stony Brook University, Stony Brook, NY 11794-3400, USA, [2]Department of Biomedical Engineering, Stony Brook University, Stony Brook, NY 11794-2580 USA and [3]Department of Materials Science and Engineering, Stony Brook University, Stony Brook, NY 11794-2275, USA

Received June 3, 2005; Revised September 26, 2005; Accepted October 14, 2005

ABSTRACT

Extracellular and intracellular barriers typically prevent non-viral gene vectors from having an effective transfection efficiency. Formulation of a gene delivery vehicle that can overcome the barriers is a key step for successful tissue regeneration. We have developed a novel core-shelled DNA nanoparticle by invoking solvent-induced condensation of plasmid DNA (β-galactosidase or GFP) in a solvent mixture [94% N,N-dimethylformamide (DMF) + 6% 1× TE buffer] and subsequent encapsulation of the condensed DNA globule in a triblock copolymer, polylactide-poly(ethylene glycol)-polylactide ($L_8E_{78}L_8$), in the same solvent environment. The polylactide shell protects the encapsulated DNA from degradation during electrospinning of a mixture of encapsulated DNA nanoparticles and biodegradable PLGA (a random copolymer of lactide and glycolide) to form a nanofibrous non-woven scaffold using the same solution mixture. The bioactive plasmid DNA can then be released in an intact form from the scaffold with a controlled release rate and transfect cells *in vitro*.

INTRODUCTION

The search for viable alternative approaches to deal with problems associated with viral DNA delivery (i.e. safety, toxicity and fate of transfected cells, etc.) has prompted many researchers to develop non-viral means of delivering genes *in vivo*. Typical non-viral approaches include naked DNA, cationic lipids formulated into liposomes and subsequent complex formation with DNA (lipoplexes), complex formation of cationic polymers with DNA (polyplexes), and collagen- or hyaluronan-based DNA gels (1). Recently, new biomaterials, such as the gene activated matrix (GAM) and biodegradable polymers (i.e. polylactide-co-glycolide, PLGA) have been developed that can serve as scaffolds for DNA delivery and tissue engineering (2,3) Even though non-viral gene delivery systems offer enhanced safety over viral systems, they are plagued with comparatively low transfection efficiencies. Non-viral gene delivery encounters many barriers, including degradation of the DNA in plasma, uptake of DNA by the reticuloendothelial system, lysosomal degradation of the DNA and lack of translocation to the nucleus (1,4). To overcome these barriers, the critical component of design formulation must be based on the fundamental understanding of the interactions between DNA and various chemical species in solution. Proper characterization of vectors thus becomes an essential step in the development of efficient non-viral gene delivery systems.

The process of DNA condensation has attracted a great deal of attention in recent years due to its biological importance in viral DNA packing, as well as in the development of gene delivery vehicles (5,6). The extended DNA chain could effectively be collapsed into a compact globule through charge neutralization by cationic polymers (7,8), polyamines and other multivalent cations, such as spermidine (9) and cobalt hexamine [$Co(NH_3)_6^{3+}$] (10). In this study, we chose the approach of solvent-induced condensation of DNA. There are two advantages of using a poor (or non-) solvent for DNA to undergo coil-to-globule transition: (i) no contamination by other unwanted species, and (ii) easy removal of solvent through evaporation. The chosen poor solvent was 94% (in volume) N,N-dimethylformamide (DMF) + 6% 1× TE buffer. It was found that DNA could remain intact in DMF for at least several days and its bioactivity was maintained.

We have designed a unique scheme that can overcome some barriers in non-viral gene delivery. Our scheme is as follows.

*To whom correspondence should be addressed. Benjamin Chu, Department of Chemistry, Stony Brook University, Stony Brook, NY 11794-3400, USA. Tel: +631 632 7928; Fax: +631 632 6518; Email: bchu@notes.cc.sunysb.edu
Present address:
Dehai Liang, Department of Polymer Science and Engineering, College of Chemistry and Molecular Engineering, Peking University, 100871 China.

Encapsulated DNA nano-particles with a core-shell structure were first created by condensing plasmid DNA in a poor solvent mixture, followed by encapsulation of the condensed DNA in a triblock copolymer of poly(lactide)-b-poly(ethylene glycol)-b-poly(lactide) (*LEL*) that formed micelles under the same solvent environment. This mixture was designed as a suitable solvent for random copolymers of lactide and glycolide (PLGA). The mixtures of encapsulated DNA and PLGA were then electrospun to form a non-woven nanofibrous and nanocomposite scaffold, whereby the solvent mixture was rapidly removed by evaporation in the jet stream during fiber formation in the electrospinning process. Thus, the plasmid DNA was preserved in the nanofibrous scaffold. As a gene delivery vehicle, the polylactide shell protected the DNA core from degradation and maintained its bioactivity during electrospinning. The encapsulated DNA could be released from the scaffold by controlled degradation of the biodegradable scaffold component (PLGA). Transfection of adhered cells could then be enhanced by sustained DNA release and immobilization in contact with adhered cells.

MATERIALS AND METHODS

Preparation of DNA and triblock polymer

pCMVβ plasmid DNA (7164 bp) encoding β-galactosidase (Clontech, Palo Alto, CA) was extracted from cultured *Escherichia coli* utilizing a Qiagen (Valencia, CA) GigaPrep DNA isolation kit. PLA-PEG-PLA triblock copolymer was synthesized by copolymerizing PEG (3.4K) and D,L-lactide at 130°C for 15 h with stannous octoate being the catalyst. The molecular weight of purified reaction product was determined by ^{1}H nuclear magnetic resonance (^{1}H NMR) and gel permeation chromatography (GPC).

Laser light scattering (LLS)

A LLS spectrometer equipped with a BI-9000 AT digital correlator and a solid-state laser (DPSS, Coherent, 200 mW and 532 nm) was used to perform static and dynamic light scattering (DLS) studies over an angular range of 20–120°. In static LLS, the angular dependence of the excess absolute time-averaged scattered intensity, known as the Rayleigh ratio $R_{vv}(\theta)$, was measured. For a very dilute solution, the weight-averaged molecular weight (M_w), the root mean square radius of gyration (R_g), and the second virial coefficient (A_2) can be obtained on the basis of

$$[HC/R_{vv}(\theta)] \approx (1/M_w)[1 + (1/3)R_g^2q^2] + 2A_2C \quad \mathbf{1}$$

where $H = 4\pi^2n^2(dn/dC)^2/(N_A\lambda^4)$ and $q = (4\pi n/\lambda)\sin(\theta/2)$ with N_A, n, dn/dC and λ being the Avogadro constant, the solvent refractive index, the specific refractive index increment and the wavelength of light in vacuum, respectively.

In dynamic LLS, the intensity–intensity time correlation function $G^{(2)}(t)$ in the self-beating mode was measured.

$$G^{(2)}(t) = A[1 + \beta|g^{(1)}(t)^2] \quad \mathbf{2}$$

where A is the measured base line, β is a coherence factor, t is the delay time and $g^{(1)}(t)$ is the normalized first-order electric field time correlation function. $g^{(1)}(t)$ is related to the line width distribution $G(\Gamma)$ by

$$g^{(1)}(t) = \int_0^\infty G(\Gamma)e^{-\Gamma t}d\Gamma \quad \mathbf{3}$$

By using a Laplace inversion program, CONTIN, the normalized distribution function of the characteristic line width $G(\Gamma)$ was obtained. The line width Γ is a function of both C and q, which can be expressed as

$$\Gamma/q^2 = D(1 + k_dC)[1 + f(R_gq)^2] \quad \mathbf{4}$$

with D, k_d and f being the translational diffusive coefficient, the diffusion second virial coefficient, and a dimensionless constant, respectively. When the concentration is extremely dilute and $R_gq << 1$, Γ/q^2 is approximately equal to D. D can be further converted into the hydrodynamic radius R_h by using the Stokes–Einstein equation:

$$D = k_BT/6\pi\eta R_b \quad \mathbf{5}$$

where k_B, T and η are the Boltzmann constant, the absolute temperature, and the viscosity of the solvent, respectively.

Measurement on d*n*/d*C*

Differential refractometer (Phoenix Precision Instruments, NY) was used to measure the dn/dC value of PLA and PEG in 94% DMF + 6% TE at 25°C. The instrument was calibrated in advance by using aqueous potassium chloride solutions. At a wavelength of 546 nm, the measured d*n*/d*C* of PLA and PEG in 94% DMF + 6% TE exhibited a value of 0.030 ml/g and 0.044 ml/g, respectively. The d*n*/d*C* values of plasmid DNA in 1× TE buffer and in 94% DMF + 6% TE were 0.17 ml/g and 0.10 ml/g, respectively.

Scaffold preparation and DNA release

DNA incorporation into electrospun scaffolds and DNA release assays from scaffold sections have been reported previously by our laboratory (11). The scaffold preparation procedures in this study were similar to those reported before. Briefly, PLA-PEG block copolymer was dissolved in N,N-dimethylformamide, to which pCMVβ plasmid (5 mg/ml, in TE Buffer) and PLGA (LA/GA = 75/25) were added. The final solution contains 94% DMF + 6% TE. Solutions and scaffolds without block copolymer (only PLGA and DNA) were prepared identically except for the omission of block copolymer. Scaffolds were electrospun at ~25 kV with a solution flow rate of 20 μl/min. The spinneret (anode) was fixed at ~15 cm above the aluminum-covered rotating collection drum (cathode).

The electrospun scaffolds were cut into 1.5 × 1.0 cm sections and each section was incubated at 37°C with 1 ml TE buffer in Eppendorf tubes. The amount of DNA released into solution was quantified by using the Pico Green Assay, where solutions were excited at 485 nm, and the emission was measured at 530 nm in a microplate reader (CytoFluor Series 4000, Perseptive Biosystems). Integrity of released DNA was determined by 0.8% agarose gel electrophoresis and visualized by ethidium bromide staining.

Cell culture and transfection

Transfection studies were conducted using the MC3T3-E1 pre-osteoblastic cell line. MC3T3 cells were maintained in

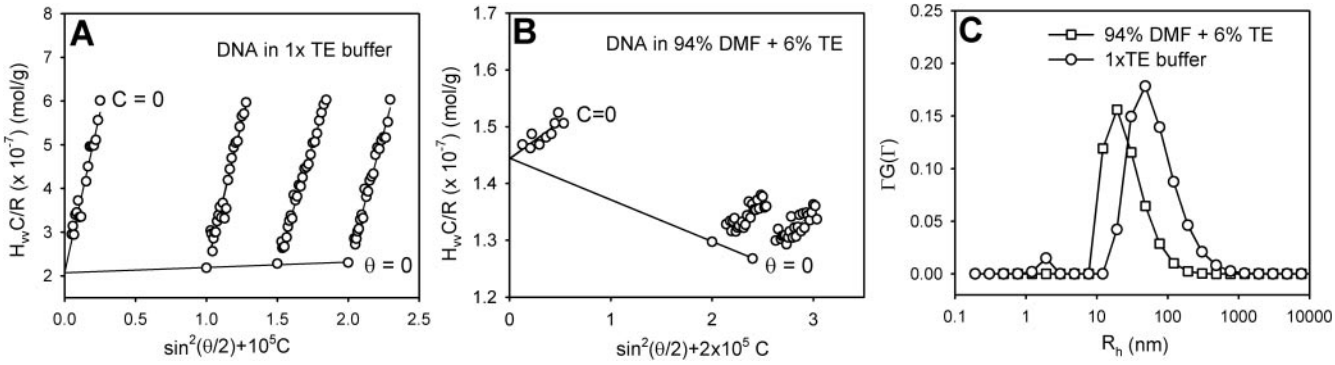

Figure 1. Condensation of plasmid DNA in 94% DMF + 6% TE studied by laser light scattering. (**A** and **B**) Shows the Zimm plots of plasmid DNA in 1× TE buffer, and in 94% DMF + 6% TE, respectively. (**C**) Shows the size distribution of DNA measured by DLS at 90° and 1.0×10^{-5} g/ml DNA concentration.

log growth phase using α-MEM supplemented with 10% fetal bovine serum (FBS) (Life Technologies, Grand Island, NY). Cells were plated at an initial density of 1×10^5 cells/well into 6-well plates, 24 h before transfection. The negative control was designated as 2 μg naked DNA added directly to cell culture solution. A positive control was constructed using the commercially available Fugene 6 transfection reagent [3:2 ratio of reagent (μl) to DNA (μg)]. Cells were incubated with two 1.5 × 1 cm sections of DNA loaded scaffolds, with and without the block copolymer. For the other set of transfection experiments with the GFP plasmid, 1×10^5 cells (20 μl) were placed directly in the center of 1.5 × 1 cm sections of PLGA/LEL and PLGA/LEL/GFP plasmid DNA scaffold (n = 3/scaffold type). Initially, the 20 μl droplet remained intact in the center of the scaffold, but it spread out to cover the entire scaffold with time (~1 h). After 1 h, the scaffold was transferred into a 12-well tissue culture plate, containing cell culture medium. After 24 h, the scaffolds were removed from the tissue culture plates and fixed with 1% formaldehyde before staining with 0.1% Nuclear Fast Red (Sigma) prepared in 5% aluminum sulfate. The scaffolds were then washed twice with distilled water, and dehydrated with an ethanol gradient (70, 95 and 100%). Finally, the scaffolds were placed on microscope slides and cells (present only on the exterior surface of the scaffold) were imaged under epi-fluorescence for the presence of GFP using a Zeiss Axiovert microscope.

RESULTS AND DISCUSSION

LLS

Both static light scattering (SLS) and DLS, was employed to monitor the changes in DNA size and conformation. Figure 1A and B show Zimm plots of pCMVβ plasmid DNA (7164 bp) encoding β-galactosidase in 1× TE buffer [10 mM Tris base and 1 mM EDTA in pure water (pH 8.0)] and in 94% DMF + 6% TE, respectively. From the Zimm plot, the weight average molecular weight (M_w), the radius of gyration (R_g) and the second virial coefficient (A_2) were obtained (Table 1). In 94% DMF + 6% TE, M_w of plasmid DNA was only slightly larger than that in 1× TE buffer. However, the R_g value was significantly reduced from 135 nm (in 1× TE buffer) to about 15 nm, suggesting the occurrence of chain collapse. A_2 was used to describe the interactions between solute and solvent. In general, A_2 is positive when a sample was dissolved in a good solvent. As expected, the value of A_2 (-3.7×10^{-4} mol cm^3 g^{-2}) became negative in 94% DMF + 6% TE because this mixture was a poor solvent for DNA. The hydrodynamic radius, R_h, obtained from the CONTIN (12) analysis of dynamic light scattering data, was also dramatically decreased from 87 nm in 1× TE buffer to about 17 nm in 94% DMF + 6% TE (Figure 1C). The relationship between the conformation of polymer chains and the R_g/R_h ratio has been well established. Typically, a random coil has an R_g/R_h value of 1.5, and a solid sphere has a value of 0.775 (13). As shown in Table 1, plasmid DNA had an R_g/R_h ratio of 1.55 in 1× TE buffer, suggesting essentially a random-coil conformation; while in 94% DMF + 6% TE, the value was about 0.88, very close to 0.775, indicating a relatively compact solid-sphere conformation.

Table 1. Physicochemical properties of plasmid DNA measured by LLS

Parameters	1× TE buffer	94% DMF + 6% TE
M_w (10^6 g/mol)	4.81 ± 0.21	6.9 ± 0.6
R_g (nm)	135 ± 6	15.2 ± 1.8
A_2 (Mol cm^3 g^{-2})	8.0×10^{-4}	-3.7×10^{-4}
D_0 (10^{-8} cm^2 s^{-1})	2.78 ± 0.13	12.4 ± 1.1
R_h (nm)	87 ± 2	17.2 ± 2.0
R_g/R_h	1.55 ± 0.09	0.88 ± 0.15

The triblock copolymer used in this study (*LEL*), was synthesized according to a known scheme (14). In brief, PEG and D,L-lactide with known ratio were mixed together and the polymerization was accomplished at 130°C for 15 h using stannous octoate as the catalyst. Before mixing plasmid DNA and *LEL* together, the behavior of *LEL* itself in 94% DMF + 6% TE was studied. With the known molecular weight of PEG block (3.4 k), the number-averaged molecular weight of PLA block could be estimated from proton NMR (data not shown), which was about 0.6 k. Therefore, the average repeating unit of each block was estimated to be $L_8E_{78}L_8$. GPC also confirmed this as the weight average molecular weight of *LEL* was about 5.9 k.

Figure 2A shows the excess scattered intensity of *LEL* at different copolymer concentrations in the same solvent mixture. No sharp increase in the scattered intensity over a range of concentrations was observed, suggesting either the absence of micelle formation or a very low critical micelle concentration. At concentrations higher than ~1×10^{-3} g/ml, *LEL* showed M_w of about 180 k (Figure 2B), a value at almost 30 times

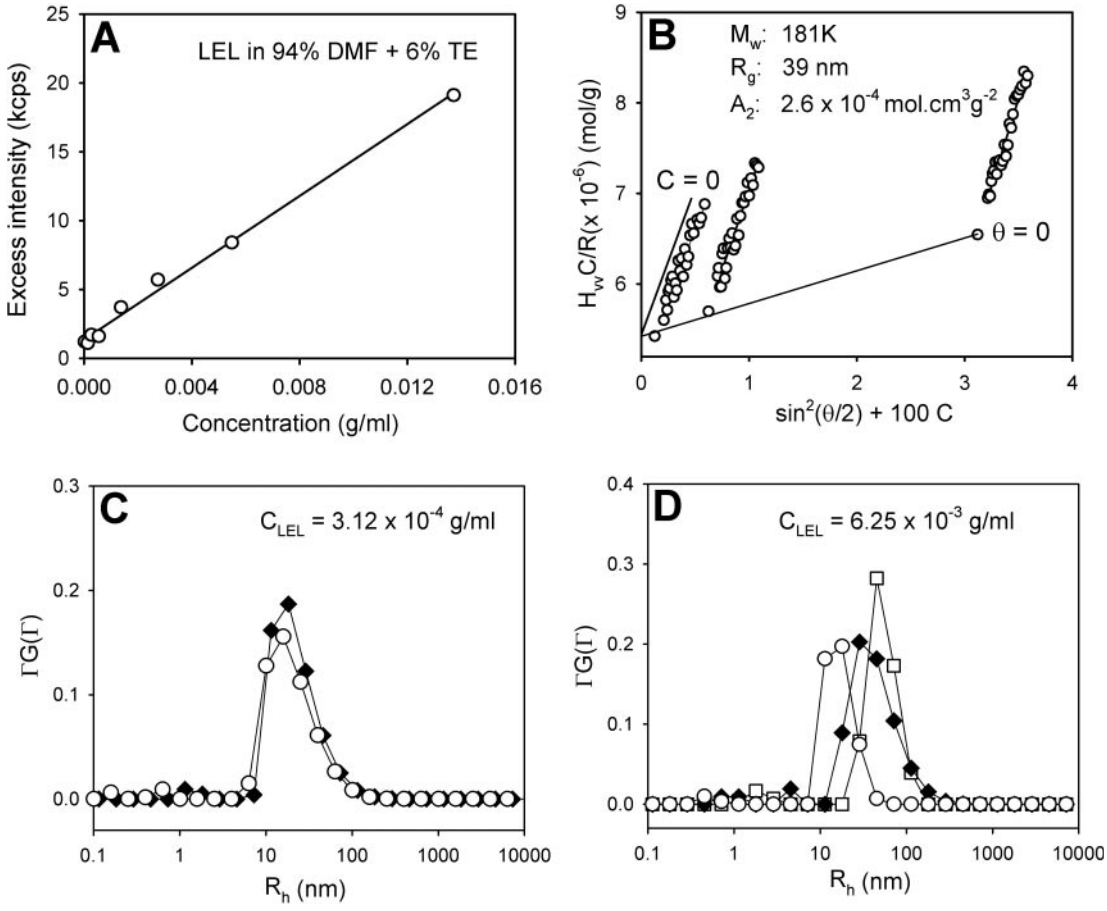

Figure 2. Encapsulation of plasmid DNA by triblock copolymer of *LEL* in 94% DMF + 6% TE. (**A**) Excess scattered intensity of *LEL* at different concentrations measured at 90°; (**B**) Zimm plot of *LEL* at concentrations of 1.25, 6.24 and 31.2 mg/ml; (**C** and **D**) CONTIN analysis of plasmid DNA (hollow circles), *LEL* (hollow squares) and their mixtures (solid diamonds) at different DNA/*LEL* weight ratio. The concentration of DNA used in panels C and D is 1×10^{-5} g/ml.

larger than that measured by GPC. The measured R_g value was 39 nm, significantly larger than the size of a polymer chain with an M_w of only 5.9 k. The hydrodynamic radius, R_h, measured from DLS (data not shown), had a value of 44 nm, very close to R_g. All these results confirmed that *LEL* chains were aggregated in 94% DMF + 6% TE at concentrations above $\sim1 \times 10^{-3}$ g/ml.

DNA (at 1×10^{-5} g/ml) was subsequently mixed with *LEL* at two different concentrations, 3.12×10^{-4} g/ml and 6.25×10^{-3} g/ml. At 3.12×10^{-4} g/ml, where *LEL* did not aggregate, the size and distribution of the DNA/*LEL* mixture were almost the same as those of plasmid DNA itself (Figure 2C). In other words, there was an insufficient amount of *LEL* to encapsulate the condensed plasmid DNA. At *LEL* concentration of 6.25×10^{-3} g/ml, a value where *LEL* already aggregated, only one 'size' with a relatively broad size distribution was observed for DNA/*LEL* in the solvent mixture (Figure 2D). The average size, however, became even smaller than that of the pure *LEL* aggregate, but larger than that of the plasmid DNA itself, indicating that a fusion of plasmid DNA and *LEL* aggregates had occurred.

The molecular scale interaction of DNA and *LEL* is depicted schematically in Figure 3. The figure also included experimental evidence for the condensation of plasmid DNA, the aggregation of *LEL* and the encapsulation of DNA by *LEL* in 94% DMF + 6% TE. Initially, after being air dried from 1× TE buffer, plasmid DNA was rod-like with a length >200 nm (Figure 3A), very close to the shape of a compact random coil with high super-helicity. Depending on the chain length and the degree of super-helicity, the DNA chain could be loose, compact or even branched. In 94% DMF + 6% TE, the DNA chain was condensed to form a much smaller globule with a diameter of ~30 nm (Figure 3B). By design, *LEL* was also aggregated in 94% DMF + 6% TE above a certain concentration, which can be explained as follows. TE is a good solvent for PEG but not for PLA. In the solution mixture, water molecules prefer to stay together with PEG blocks instead of PLA blocks. Even though DMF is a good solvent for both PEG and PLA, their solubility in the solvent mixture could be different, causing the triblock copolymer molecules to aggregate. The average diameter of the aggregates was around 80 nm at concentrations above 1×10^{-3} g/ml (Figure 2B). Given that the bond lengths of C-C and C-O are 0.154 nm and 0.143 nm, respectively, the maximum backbone length of $L_8E_{78}L_8$ should be <30 nm even if the polymer chain were fully stretched. Therefore, each *LEL* aggregate could contain more than one PEG domain, while the PEG domains should contain most of the water molecules.

Upon mixing with condensed DNA, which is hydrophilic, such PEG/water domains could serve as a 'shelter' for the

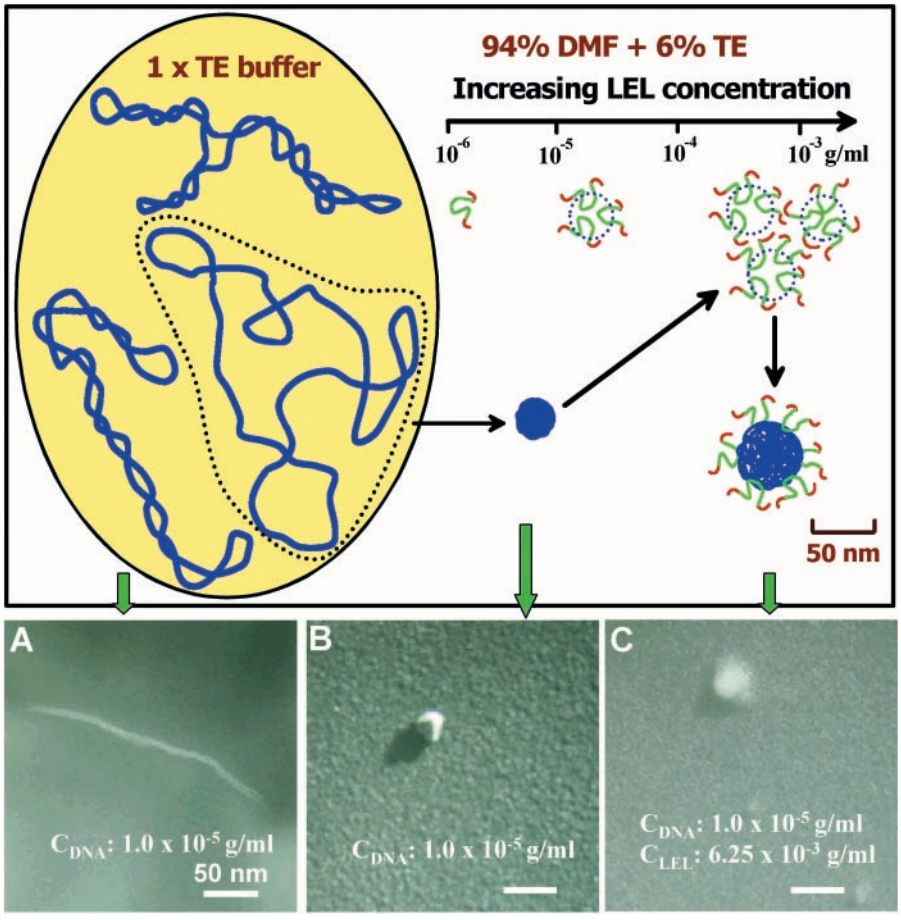

Figure 3. Schematic presenting the condensed plasmid DNA, the aggregation of *LEL* and the encapsulation of DNA by *LEL*. (**A**–**C**) Shows TEM images of DNA in 1× TE buffer, DNA in 94% DMF + 6% TE and encapsulated DNA in 94% DMF + 6% TE, respectively.

plasmid DNA. As DNA and PLA were essentially incompatible, one expect that the *LEL* chains could accommodate the condensed DNA particles to form a core-shell structure. In other words, the DNA particles were encapsulated by *LEL*, which was exactly what we observed by laser light scattering results as well as TEM imaging at various stages (super coiled plasmid, condensed plasmid and encapsulated DNA nanocomposite particle, Figure 3A–C). After mixing with 6.25×10^{-3} g/ml *LEL*, the size increased and the edge became blurred mainly due to the short *LEL* chains acting as a protective shell for the condensed DNA (Figure 3C). All of these experimental results were in agreement with our hypothesis. The core-shell structure, as shown in Figure 3, was quite different from the DNA structure, typically toroids (15,16) and rods (17), formed in aqueous solutions upon mixing with multivalent cations, including cationic polymers and polyamines (6).

Formulation of DNA particles into electrospun nanofibers

DNA nanoparticles with a core-shell structure were created in two steps: condensation and encapsulation. The main objective for the PLA shell was to produce an effective protective shell for the DNA globules during the electrospinning process. Moreover, such DNA particles could be incorporated into non-woven nanofibrous PLGA scaffolds for controlled release (11). The electrospun nanofibrous scaffolds possess many unique properties, including high surface-to-volume ratio, appropriate porosity and malleability, to conform to a wide variety of sizes and shapes, which make them superior substrates for tissue engineering (18) as well as for the delivery of cells, and bioactive agents, including drugs (19,20), protein (21) and DNA (11,22).

Based on laser light scattering results, PLGA (M_w = 75 k, LA/GA = 75/25) and plasmid DNA with or without *LEL* were formulated into a viscous solution, and the scaffold was produced by electrospinning. Following construction of the PLGA/DNA scaffolds with and without *LEL*, a comparison of scaffold morphology was made via SEM. Figure 4A shows an example of PLGA scaffolds having ~10% w/w *LEL* and DNA with a *LEL*/DNA weight ratio of more than 150. The scaffolds contained thin and fairly uniformly distributed submicron diameter fibers. The SEM image of PLGA scaffold without *LEL* (data not shown) showed no visual difference in the overall morphology, porosity and fiber diameter. Thus, the presence or absence of a block copolymer has little effect on the overall structural morphology of these scaffolds. Upon the removal of remaining trace amounts of solvent (94% DMF + 6% TE) under vacuum, the ability of scaffolds

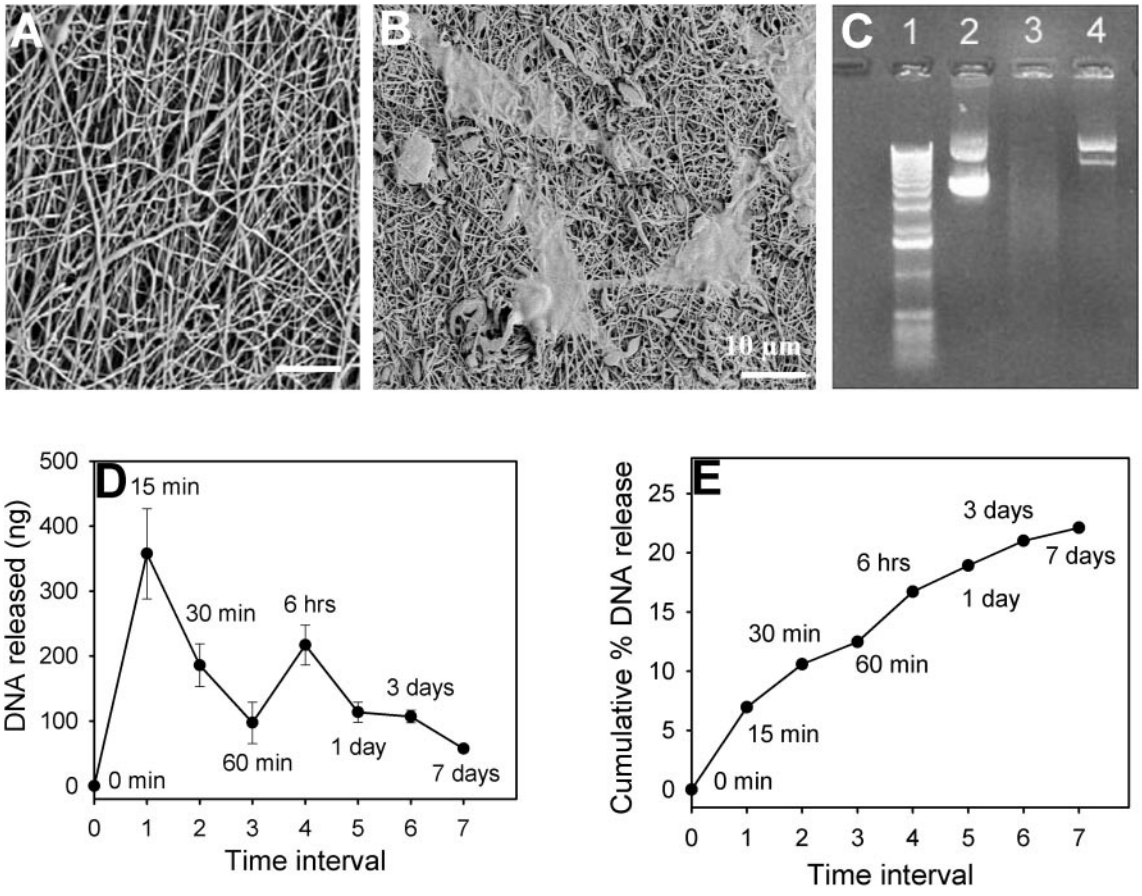

Figure 4. Incorporation and release of plasmid DNA from electrospun nanofibrous PLGA-based scaffolds. (**A**) SEM image of electrospun PLGA scaffold with *LEL* added; (**B**) Cellular adhesion on PLGA scaffold containing *LEL* and encapsulated DNA; (**C**) Gel electrophoresis of DNA samples, lane 1 ladder, lane 2 control plasmid, lanes 3 and 4 released (4 h) plasmid DNA from PLGA scaffold without/with *LEL*; (**D** and **E**) Shows the controlled release of DNA from PLGA scaffold with *LEL*.

to support cellular (pre-osteoblastic MC3T3) adhesion was tested, which results are illustrated in Figure 4B.

DNA released from the scaffold was analyzed via the use of a Pico Green assay and agarose gel electrophoresis. Results showed that the DNA-containing scaffolds without the block copolymer contained degraded DNA (as a result of the electrospinning process), which is shown in lane 3 of Figure 4C where the degraded DNA appeared as a 'smear' spanning the length of the gel lane. In contrast, in the presence of block copolymer, the DNA released from the scaffold was essentially intact structurally, with no apparent degradation (lane 4 of Figure 4C). Lane 2 indicates unincorporated intact plasmid DNA, which was used as a positive control. Figure 4C demonstrates that the core-shell structure has protected the condensed DNA globule from degradation during the electrospinning process. More importantly, the structural integrity of the plasmid DNA was preserved.

To clarify how the DNA/*LEL* nanoparticles were incorporated in the PLGA fibers, the sustained release of intact DNA from PLGA scaffold was measured over a 7 day time period via the Pico Green assay. Figure 4D and E illustrate the amount of DNA released from the scaffold decreased with time. After 7 days, a large fraction (~75%) of the DNA remained in the partially degraded scaffold. Thus, the DNA release profile could be primarily coupled with the scaffold degradation profile. It is noted that the structural integrity of the encapsulated and dried (after evaporation of solvent in the scaffold from electrospinning) DNA remained intact. During the release process, where a dry scaffold was immersed into an aqueous solution, *LEL* aggregates were disassembled and the *LEL* chains would likely form a flower-like micelle with PLA being the core and PEG being the corona (data not shown). This inside-out transformation would instantly cause the release of the encapsulated DNA. Therefore, the DNA release rate could also be influenced by the diffusion of aqueous solution into the PLGA scaffold. The biodegradation of the scaffold is also partially affected by the presence of encapsulated DNA. As only ~25% DNA was released in 7 days, a large amount of the encapsulated DNA was successfully incorporated inside the 'dry' PLGA fiber. We could modulate the DNA release profile by tuning the chemical composition of PLGA, i.e. the LA/GA ratio (23).

After forming the scaffold, a small portion of the encapsulated DNA could be attached on and near the fiber surface. These DNA/*LEL* particles were quickly released upon dipping the scaffold into an aqueous solution. The release of encapsulated DNA inside the PLGA could depend on its location in the fiber, as clearly illustrated by the two release rates (Figure 4D). The remaining portion of these DNA/*LEL* particles could not be released until the biodegradable scaffold,

whose degradation rate could be controlled, was degraded further.

Transfection of released DNA

There was a difference in the structural quality of the released DNA from the two types of scaffolds (with and without block copolymer). We sought to determine whether these differences could be translated into the bioactivity of the released DNA. Results from transfection experiments using pre-osteoblastic MC3T3 cells and sections of scaffolds immersed in culture medium, are presented in Figure 5. The results clearly indicate that no transfection was evident in cell populations incubated with PLGA and DNA scaffolds without *LEL* (Figure 5A). This lack of transfection could be correlated with the fact that the DNA released from the scaffold without the block copolymer was degraded (Figure 4C, lane 3). In contrast, transfection was observed from scaffolds where 10% *LEL* block copolymer was

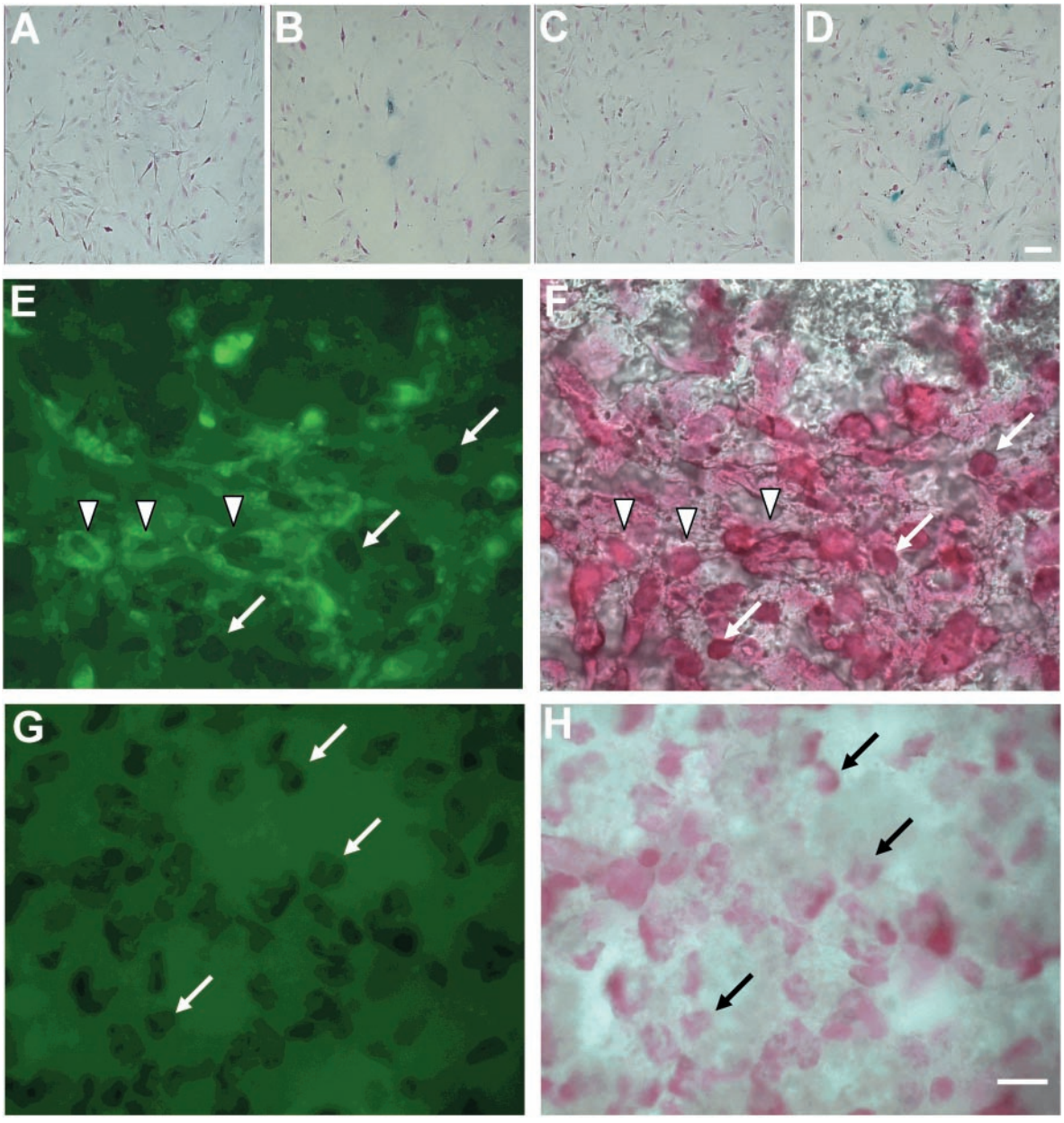

Figure 5. Transfection of MC3T3 cells by nanofibrous electrospun scaffolds. (A–D) shows the transfection of DNA released from PLGA without *LEL* (**A**), with *LEL* (**B**) and the negative (**C**) and positive (**D**) controls. Panels E–H show the increased transfection by plating MC3T3 cells directly on a GFP plasmid DNA containing scaffold. (**E**) Fluorescent image of cells on GFP plasmid DNA containing PLGA/10% block copolymer scaffold 24 h post-plating. Arrowheads indicate representative transfected GFP-expressing cells and arrows indicate non-transfected cells. (**F**) Light micrograph of cells (shown in E) stained with nuclear fast red. Arrowheads and arrows indicate identical cells in E. (**G**) Fluorescent image of cells on a control scaffold containing no DNA and indicating no fluorescent (green) cells (arrow). (**H**) Light micrograph of cells (shown in G) stained with nuclear fast red. Arrow indicates identical cells in G. This transfection efficiency reflected that of cells present only on the exterior surface of the scaffold and not for all cells within the scaffold.' Scale bar: 100 μm in Panels A–D, 10 μm in panels E–H.

incorporated (Figure 5B). Compared with naked DNA that showed no transfected cells, (Figure 5C), the PLGA/*LEL* scaffold with encapsulated DNA enhanced transfection, albeit at very low levels, is <1%. An equivalent amount of DNA complexed with the transfection reagent, Fugene, resulted in ~35% transfection efficiency (Figure 5D).

The low level (<1%) transfection efficiency obtained could be due to the fact that the DNA/*LEL* particles disassembled in an aqueous solution. Thus, we reasoned that a more appropriate way of indicating transfection efficiency was warranted. Instead of immersing sections of scaffolds into a culture dish with a growing monolayer of MC3T3 cells, we plated cells directly onto a scaffold containing a green fluorescence protein (GFP) DNA plasmid. Results from this experiment showed a dramatic increase in transfection efficiency as seen in Figure 5E and F (note that this transfection efficiency reflects that of cells present on only the exterior surface of the scaffold and not for all cells within the scaffold). In contrast, no green cells were apparent in a scaffold without any GFP DNA, as expected (Figure 5G and H). The increase in DNA transfection occurred probably in two ways: (i) the scaffold brought cells closer to the released DNA by allowing cell adhesion directly onto the nanofibers, and (ii) the released DNA maintained a relatively higher concentration around the cell surface due to its immobilization (24), enabling greater levels of DNA to enter the cells.

Together with our previous studies (11), these results demonstrate that by understanding and capitalizing on the molecular interactions of block copolymers and plasmid DNA in solution, novel structures and additional functionality can emerge. A deeper understanding on the molecular self-assemblies and the electrospinning process has enabled us to develop an effective gene delivery vehicle. In the present case, *in vitro* gene delivery to cells was accomplished by attracting the cells to a scaffold that was capable of supporting cellular adhesion. Thus, the incorporation of a homing device could be of secondary importance. The volume contraction of a condensed DNA molecule was of the order of a 1000-fold, although less than what a virus could accomplish. Nevertheless, it permitted us to encapsulate and to protect the DNA plasmid for incorporation into electrospun nanofibrous scaffolds. Finally, these scaffolds with their network structures reduced the mobilization of released DNA before transfection. Thus, control of the fabricated gene delivery scaffold could be developed in terms of the scaffold morphology, material properties and release profiles, ultimately leading towards improved transfection efficiency.

ACKNOWLEDGEMENTS

We thank Christine Falabella for help with tissue culture. Ben Chu gratefully acknowledges the support of this work by the National Science Foundation (DMR 9984102 and 0454887), and in particular, for the creativity extension award that permits him to pursue this new direction. Funding to pay the Open Access publication charges for this article was provided by NSF (DMR 0454887).

Conflict of interest statement. None declared.

REFERENCES

1. Brown,S.A. and Uchegbu,I.F. (2001) Gene delivery with synthetic (non-viral) carriers. *Int. J. Pharm.*, **229**, 1–21.
2. Shea,L.D., Smiley,E., Bonadio,J. and Mooney,D.J. (1999) DNA delivery from polymer matrices for tissue engineering. *Nat. Biotechnol.*, **17**, 551–554.
3. Fang,J., Zhu,Y.Y., Smiley,E., Bonadio,J., Rouleau,J.P., Goldstein,S.A., McCauley,L.K., Davidson,B.L. and Roessler,B.J. (1996) Stimulation of new bone formation by direct transfer of osteogenic plasmid genes. *Proc. Natl Acad. Sci. USA*, **93**, 5753–5758.
4. Pouton,C.W. and Seymour,L.W. (2001) Key issues in non-viral gene delivery. *Adv. Drug Deliv. Rev.*, **46**, 187–203.
5. Bloomfield,V.A. (1996) DNA condensation. *Curr. Opin. Struct. Biol.*, **6**, 334–341.
6. Vijayanathan,V., Thomas,T. and Thomas,T.J. (2002) DNA nanoparticles and development of DNA delivery vehicles for gene therapy. *Biochemistry*, **41**, 14085–14094.
7. Wagner,E., Zenke,M., Cotten,M., Beug,H. and Birnstiel,M.L. (1990) Transferrin-polycation conjugates as carriers for DNA uptake into cells. *Proc. Natl Acad. Sci. USA*, **87**, 3410–3414.
8. Dunlap,D.D., Maggi,A., Soria,M.R. and Monaco,L. (1997) Nanoscopic structure of DNA condensed for gene delivery. *Nucleic Acids Res.*, **25**, 3095–3101.
9. Saminathan,M., Thomas,T., Shirahata,A., Pillai,C.K.S. and Thomas,T.J. (2002) Polyamine structural effects on the induction and stabilization of liquid crystalline DNA: potential applications to DNA packaging, gene therapy and polyamine therapeutics. *Nucleic Acids Res.*, **30**, 3722–3731.
10. Thomas,T.J. and Bloomfield,V.A. (1983) Collapse of DNA caused by trivalent cations: pH and ionic specificity effects. *Biopolymers*, **22**, 1097–1106.
11. Luu,Y.K., Kim,K., Hsiao,B.S., Chu,B. and Hadjiargyrou,M. (2003) Development of a nanostructured DNA delivery scaffold via electrospinning of PLGA and PLA-PEG block copolymers. *J. Control Release*, **89**, 341–353.
12. Provencher,S.W. (1982) CONTIN: a general purpose constrained regularization program for inverting noisy linear algebraic and integral equations. *Comput. Phys. Commun.*, **27**, 229–242.
13. Burchard,W. (1983) Static and dynamic light scattering from branched polymers and biopolymers. *Adv. Polym. Sci.*, **48**, 1–124.
14. Kim,K., Chung,S., Chin,I., Kim,M. and Yoon,J. (1999) Crystallization behavior of biodegradable amphiphilic poly(ethylene glycol)-poly(L-lactide) block copolymers. *J. Appl. Polym. Sci.*, **72**, 341–348.
15. Golan,R., Pietrasanta,L.I., Hsieh,W. and Hansma,H.G. (1999) DNA toroids: stages in condensation. *Biochemistry*, **38**, 14069–14076.
16. Vijayanathan,V., Thomas,T., Antony,T., Shirahata,A. and Thomas,T.J. (2004) Formation of DNA nanoparticles in the presence of novel polyamine analogs: a laser light scattering and atomic force microscopic study. *Nucleic Acids Res.*, **32**, 127–134.
17. Rouzina,I. and Bloomfield,V.A. (1998) DNA bending by small, mobile multivalent cations. *Biophys J.*, **74**, 3152–3164.
18. Yoshimoto,H., Shin,Y.M., Terai,H. and Vacanti,J.P. (2003) A biodegradable nanofiber scaffold by electrospinning and its potential for bone tissue engineering. *Biomaterials*, **24**, 2077–2082.
19. Verreck,G., Chun,I., Rosenblatt,J., Peeters,J., Dijck,A.V., Mensch,J., Noppe,M. and Brewster,M.E. (2003) Incorporation of drugs in an amorphous state into electrospun nanofibers composed of a water-insoluble, nonbiodegradable polymer. *J. Control Release*, **92**, 349–360.
20. Kim,K., Luu,Y.K., Chang,C., Fang,D., Hsiao,B.S., Chu,B. and Hadjiargyrou,M. (2004) Incorporation and controlled release of a hydrophilic antibiotic using poly(lactide-co-glycolide)-based electrospun nanofibrous scaffolds. *J. Control Release*, **98**, 47–56.
21. Amsden,B.G. and Goosen,M.F.A. (1997) An examination of factors affecting the size, distribution and release characteristics of polymer microbeads made using electrostatics. *J. Control Release*, **43**, 183–196.
22. Zeng,J., Xu,X., Chen,X., Liang,Q., Bian,X., Yang,L. and Jing,X. (2003) Biodegradable electrospun fibers for drug delivery. *J. Control Release*, **92**, 227–231.
23. Zong,X., Kim,K., Ran,S., Fang,D., Hsiao,B.S. and Chu,B. (2003) *Biomacromolecules*, **4**, 416–423.
24. Segura,T., Volk,M.J. and Shea,L.D. (2003) Substrate-mediated DNA delivery: role of the cationic polymer structure and extent of modification. *J. Control Release*, **93**, 69–84.